



Supporting Online Material for

***Arabidopsis* Stomatal Initiation Is Controlled by MAPK-Mediated Regulation of the bHLH SPEECHLESS**

Gregory R. Lampard, Cora A. MacAlister, Dominique C. Bergmann*

*To whom correspondence should be addressed. E-mail: dbergmann@stanford.edu

Published 14 November 2008, *Science* **322**, 1113 (2008)
DOI: 10.1126/science.1162263

This PDF file includes:

Materials and Methods

SOM Text

Figs. S1 to S11

References

Supplemental Materials

Materials and methods:

Plant materials: Col-0 was used as wildtype unless otherwise noted. Lines and alleles used in this study were as follows: *mpk3* (SALK_100651) *mpk6* (SALK_074003) *erl1-2;erl2-1 (1)*, *spch-3 (2)*, *tmm-1 (3)*, *CA-YDA (4)*, *sdd1-1 (5)*, *MUTEpro::GFP (2)* and *TMMpro::TMM-GFP (6)*.

Construction of SPCH variants:

In the 3 SPCH deletion constructs, $\Delta 93$, $\Delta 49$ and $\Delta 31$, residues 171 to 264, 171 to 220 and 236 to 267, respectively were deleted and replaced by a penta-alanine linker region using primers indicated in Table 1. The resulting SPCH Δ pENTR vectors were recombined into pMDC43 (7) for expression of N-terminal GFP-fusions with the 35S promoter. For expression with the SPCH promoter, a 2.5 Kb NotI digested purified SPCH promoter fragment (2) was ligated into the NotI site in pENTR and recombined into pMDC99 or pMDC107 for GFP fusion (7). SPCH variants with specific S/T residue alterations were constructed from a SPCH pENTR template using the QuikChange XL Site-Directed Mutagenesis Kit (Stratagene, La Jolla, CA) according to the manufacturer's protocols using oligonucleotides listed in Table 1. The SPCH promoter was inserted into SPCH S/T>A pENTR constructs as described and subsequent S/T>A variants were recombined into pHGY (8) for transformation of and subsequent expression in Arabidopsis.

Table 1: Primer table for SPCH and MAPK variants		
Primer name	sequence	Use
SPCHindel2	GCTGCAGCCGCCGTTAGTAGTAACCATGAG	to generate SPCH Δ 93
SPCHindel1	GGCTGCAGCGGCTAGGACTTCGGCGTAGGT	
SPCHindel3	GCTGCAGCCGCCTACCGGGCCATTCCACCG	to generate SPCH Δ 49
SPCHindel1	GGCTGCAGCGGCTAGGACTTCGGCGTAGGT	
SPCHpd1	(ggctgcagcggc)aagcggaggctgtggat	to generate SPCH Δ 31
SPCHpd2	GCTGCAGCCGCCAACCATGAGAGTAGTGTG	
gatestart	(cacc)ATGCAGGAGATAATACCGGA	SPCH cDNA cloning primers
SPCHro	cgcgcagaatgtttgctgaa	
SPCH 93AA/49AA insert F	CACCCTGGTTCGCGTGGATCCAGCCCCGAGAGTGTCCCGAGCCCTC	Fragment for MAPK assay
SPCH 93AA insert R	TTATGAAGGAGATGAAGAAGATGA	
SPCH 49AA insert F	TTATGGGCTTGTGGCTGAGGTG	
S193A F	AGCCCAAGAAAACCGCCTCTTGCCCCGCGCATCAACCACCACCAG	S/T>A conversions
S193A R	CTGGTGGTGGTTGATGCGCGGGGCAAGAGGCGGTTTTCTTGGGCT	
S211A F	CACCTACTTCTCCCTCCCATAGCTCCTCGAACACCTCAGCCAACA	
S211A R	TGTTGGCTGAGGTGTTTCGAGGAGCTATGGGAGGGAGAAGTAGGTG	
T214A F	CTCCCTCCATAAGTCCTCGAGCACCTCAGCCAACAAGCCCATAC	
T214A R	GTATGGGCTTGTGGCTGAGGTGCTCGAGGACTTATGGGAGGGAG	
S219A F	CCTCGAACACCTCAGCCAACAGCCCCATACCGGGCCATTCCACCG	
S219A R	CGGTGGAATGGCCCCGTATGGGGCTGTTGGCTGAGGTGTTTCGAGG	
S255A F	TTAGGAGATCCACCTCCATACGCTCCTGCTTCATCTTCTCATCT	
S255A R	AGATGAAGAAGATGAAGCAGGAGCGTATGGAGGTGGATCTCCTAA	
S211A T214A S219A F	CTCCCATAGCTCCTCGAGCACCTCAGCCAACAGCCCCATACCGGGCCATTCC	
S211A T214A S219A R	GGAATGGCCCCGGTATGGGGCTGTTGGCTGAGGTGCTCGAGGAGCTATGGGAG	
MPK3F	CACCCTGGTTCGCGTGGATCCATGAACACCGGCGGTGGCCA	in vitro kinase assay
MPK3R	CTAACCGTATGTTGGATTGAGT	

MPK6F	CACCCTGGTCCGCGTGG ATCCATGGACGGTGGTTCAGGTCA
MPK6R	CTATTGCTGATATTCTGGATTGA

Generation and purification of bacterially expressed proteins

MPK3 and MPK6 were amplified from Arabidopsis cDNA using MPK3F/R and MPK6F/R primer combinations (Table 1) using Accuprime *Pfx* DNA polymerase (Invitrogen, Carlsbad, CA). Subsequent amplified products were cloned into the pENTR-D-TOPO (Invitrogen, Carlsbad, CA) according to manufacturer's protocols. MPK3F and MPK6F primers were designed to include an in-frame thrombin cleavage site (CTG GTT CCG CGT GGA TCC/ LVPRGS) to allow for subsequent removal of the GST-Tag. Sequences encoding MPK3 and MPK6 and SPCH variants in pENTR were recombined into the *E. coli* expression vector pDEST15 (Invitrogen, Carlsbad, CA) and transformed into *E. coli* BL21 cells. GST-tagged proteins were purified batch-style using glutathione-Sepharose 4B beads (GE Healthcare, Piscataway, NJ) following standard procedures. Elution of recombinant protein was carried out using two successive ten minute incubations in one ml elution buffer, pooled and stored at -80°C until further use. Where specified, MPK3 and MPK6 proteins were eluted via cleavage with thrombin protease (GE Healthcare, Piscataway, NJ) for two hours according to manufacturer's protocols.

In vitro Kinase Assays

In vitro kinase assays to assess the ability of MPK3 or MPK6 to phosphorylate specific SPCH variants were performed based on that reported by (9) as follows: 250 ng of recombinant MAPK and 1 µg SPCH variant substrate were diluted to a total volume of 25 µL in 10X kinase buffer (25 mM Tris HCl, pH 7.5; 1 mM EDTA; 1 mM EGTA; 1 mM DTT; 5 mM MgCl₂; 25 mM ATP; 5mM β-glycerophosphate; 0.1 mM sodium orthovanadate; 1X protease inhibitor (Sigma-Aldrich, St. Louis, MO)) with MnCl₂ to auto-activate the MAPK (9). Each reaction was spiked with 5 µCi γ-³²P-ATP (Perkin Elmer, Waltham, MA) and incubated at 30°C for thirty minutes. Reactions were stopped by the addition of 6X Laemmli buffer and incubating at 75°C for ten minutes. Samples were resolved by SDS-PAGE gels and the gels were dried prior to exposure to film to detect incorporation of radioactive label.

Microscopy

DIC images were used for qualitative and quantitative examination of epidermal phenotypes on material cleared in 70% ethanol and then overnight in Hoyer's solution (10) using protocols and equipment in (2). Confocal images were taken with a Leica SP5 with excitation/emission spectra of 488/505-520 for GFP, 514/520-540 for YFP and 565/580-610 for propidium iodide counterstaining. Images were processed in ImageJ (NIH).

Scoring of phenotypes, rescue and SPCH-GFP/YFP expression patterns.

To assay the effects of SPCH variant expression on development, we aimed to have equivalently expressed lines. To this end, 2.5 KB of the endogenous 5' SPCH sequence was used as a common promoter. However, as expression of some SPCH variants induces the production of cells that express SPCH, it is not possible to find lines with equivalent SPCH RNA or protein expression across all genotypes. We have instead chosen to follow representative lines chosen from at least 12 T2s (and up to 40 lines for some) for each genotype. For each deletion and S/T>A variant two lines with median phenotypes and GFP/YFP expression were chosen for analysis. In the case of Δ93, Δ49, SPCH S/T>A1-5 and SPCH S/T>A1-4, many of the T1 plants were inviable and sterile. At least 24 T1s were also assayed from each of these lines. All phenotypes were scored on equivalently staged plants and images were taken of the basal quadrant of the cotyledon or leaf in the region between the midvein and leaf margin. For scoring phenotypes in Fig 3, cells in 6-12 0.25 mm² regions were counted for each genotype and the means calculated. Following confirmation of normality by normal probability plots, the data were subjected to one-way analysis of variance using the R statistical computing software, p-value=7.845e-15 for non-stomatal cells and 1.916e-14 for stomata. Significant differences between the full length SPCH values and each of the constructs were determined using Dunnett's test with a joint confidence coefficient of P=99% (11).

The effect of SPCH and $\Delta 49$ expression in *sddl* and *erl1;erl2* was quantified for 5 0.25mm² regions by determining the stomatal density and fraction of stomata in direct contact. Significant differences were determined by analysis of variance as above and Tukey's HSD test. The addition of the transgenes did not significantly change these values in the *sddl* background, but they were significantly higher in the *erl1;erl2* background. Suppression of *tmm-1; SPCHpro::SPCH-GFP* by *CA-YODA* was assayed by crossing *tmm-1; SPCHpro::SPCH-GFP; E1728 (2)* to *CA-YDA/+*. In the F2 generation, *SPCHpro::SPCH-GFP; E1728* was selected for on HygromycinB/Kanamycin plates. Resistant seedlings were scored for excessive hypocotyl stomata (the phenotype of *tmm-1; SPCHpro::SPCH-GFP*). 12 seedlings with this phenotype were selected, planted and scored for the presence of *CA-YDA* after bolting. None of the 12 carried the *CA-YDA* transgene. *35S::GFP-SPCH* and *35S::GFP-SPCH $\Delta 49$* were introduced into the *CA-YDA* background by Agrobacterium mediated transformation of heterozygous *CA-YDA* plants. Transformants were selected on HygromycinB. T2 seedlings were scored for *CA-YDA* by the absence of stomata as well as by the additional *CA-YDA* phenotypes including short roots and fused and supernumerary cotyledons.

Ability to rescue the null *spch-3* phenotype was assayed by transformation of the construct in question into a *spch-3* heterozygous background. Lines segregating the *spch-3* phenotype were identified by microscopic examination of 10-14 dpg cleared T2s and the number of wild type and *spch* mutant phenotype seedlings (seedlings devoid of stomata) was counted. These results were analyzed using the R statistical analysis software by chi-squared test. If the construct failed to rescue the stomatal production defect in *spch-3* the expected segregation ratio for the mutant phenotype would be 0.25, this would be reduced to 0.0625 if the construct is able to rescue. The full length SPCH under both 35S and native promoters was previously shown to rescue the *spch-3* mutation (2). All rescue data reported in Fig. S6 were significant ($p \leq 0.05$) and at least 2 (usually 4) T2 lines were tested for each construct. Both the ability to make stomata and the ability to undergo asymmetric cell divisions were assayed by the appearance of cells in 10-14 dpg cotyledons and leaves.

Identification of PEST domain.

SPCH protein was run through tools on the online PEST domain prediction site <http://www.at.embnat.org/toolbox/pestfind>. A score of +5 or higher in from this program is considered a strong prediction of a PEST domain.

Mass Spectrometry

Following *in vitro* kinase assays between MPK3 and SPCH MPKTD or MPK6 and SPCH MPKTD, proteins were separated by SDS-PAGE and coomassie stained gel bands of the SPCH MPKTD protein were excised and digested using trypsin as in (12) with the additional use of a MS friendly surfactant (Protease Max, Promega, WI.). For the enriched phosphopeptide LC MSMS runs, the extracted peptides were enriched using a swellgel gallium metal phosphopeptide enrichment kit commercially available (Thermo Scientific, Waltham, MA). The enrichment procedure was followed as suggested, with the only exception in that the enrichment buffer contained 2% lactic acid (w/v) (13). The digest was done in triplicate with three different gel bands. Each of these digests was run in duplicate providing 6 LC MSMS runs all providing consistent results and phosphopeptide determination.

Nano reversed phase HPLC was done using an Eksigent 2D nanoLC (Eksigent, Dublin, CA) with buffer A consisting of 0.1 % formic acid in water and buffer B 0.1 % formic acid in acetonitrile. A fused silica column self packed with duragel C18 (Peeke, Redwood City, CA) matrix was used with a linear gradient from 5 % B to 40 % B over 60 minutes at a flow rate of 450 nL/minute. The nanoHPLC was interfaced with an Advion Nanomate (Ithaca, NY) for nanoESI into the mass spectrometer. The mass spectrometer was a LCQ Deca XP Plus (Thermo Scientific) which was set in data dependent acquisition mode to perform MS/MS on the top three most intense ions with a dynamic exclusion setting of two. The DTA files were extracted from the raw data using the bioworks browser (Thermo Scientific). Because the gel bands only contained truncated SPCH protein and the activating kinase, the SPCH sequence was specifically searched using Sequest allowing for oxidation on methionine and phosphorylation on serine, threonine and tyrosine amino acids. All peptides with a XCorr less than 2.5 were discarded. Additionally, the same extracted DTA files were searched against the NCBI Arabidopsis thaliana database using Mascot allowing for the same fore mentioned modifications. In most cases

the suggested phosphopeptides were found in both the Sequest and Mascot searches. All MSMS spectra suggesting phosphorylation modification were manually validated.

Supplemental References

1. E. D. Shpak, J. M. McAbee, L. J. Pillitteri, K. U. Torii, *Science* 309, 290 (2005).
2. C. A. MacAlister, K. Ohashi-Ito, D. C. Bergmann, *Nature* 445, 537 (2007).
3. M. Yang, F. D. Sack, *Plant Cell* 7, 2227 (1995).
4. W. Lukowitz, A. Roeder, D. Parmenter, C. Somerville, *Cell* 116, 109 (2004).
5. D. Berger, T. Altmann, *Genes Dev.* 14, 1119 (2000).
6. J. A. Nadeau, F. D. Sack, *Science* 296, 1697 (2002).
7. M. D. Curtis, U. Grossniklaus, *Plant Physiol.* 133, 462 (2003).
8. M. Kubo et al., *Genes Dev.* 19, 1855 (2005).
9. T. Feilner et al., *Molecular & Cellular Proteomics* 4, 1558 (2005).
10. C. M. Liu, D. W. Meinke, *Plant J.* 16, 21 (1998).
11. C. W. Dunnett, *Biometrics* 20, 482 (1964).
12. A. Shevchenko; H. Tomas; Havlis, J; et al. *Nature protocols* 1, 2856 (2006)
13. N. Sugiyama; T. Masuda ; Shinoda, K; et al. *Molecular & Cellular Proteomics* 6, 1103 (2007)
14. L. J. Pillitteri, N. L. Bogenschutz, K. U. Torii, *Plant Cell Physiol.* 49, 934 (2008).

Supplemental Text

Analysis of Mass Spectrometry Data

The SPCH MPKTD was subjected to *in vitro* kinase assays in combination with either MPK3 or MPK6 as previously described with the exception that 200 μ M ATP was used in place of 32 P-ATP. Following separation by SDS-PAGE and excision of coomassie stained bands containing SPCH MPKTD, tryptic peptides were examined to identify specific residues that were phosphorylated. Peptides containing three out of the five high stringency MAPK targets sites (sites 1-3) were identified by these analyses methods and each site is phosphorylated by MPK3 and/or MPK6. Site 1 was identified only in MPK6 analyses due to the presence of miscleaved tryptic peptides that were not found in the MPK3 samples. Thus, there are no data pertaining to the ability of MPK3 to phosphorylate site 1. Similarly, phosphorylation data for site 3 was retrieved from miscleaved peptides found only in MPK3 containing assays. Site 4 is situated on a peptide that is too short to be identified; it is found on miscleaved peptides, however, on these it is situated too close to the cleavage site to obtain reliable phosphorylation data. Conversely, site 5 is situated on a peptide too long to be detected. Phosphorylation of additional -SP- motifs (S177 by MPK3 and S186 by both MPK3 and MPK6) was also detected, explaining the ability to detect 32 P incorporation in *in vitro* kinase assays examining the ability of MPK3 or MPK6 to phosphorylate the SPCH 1-5 S/T>A variant.

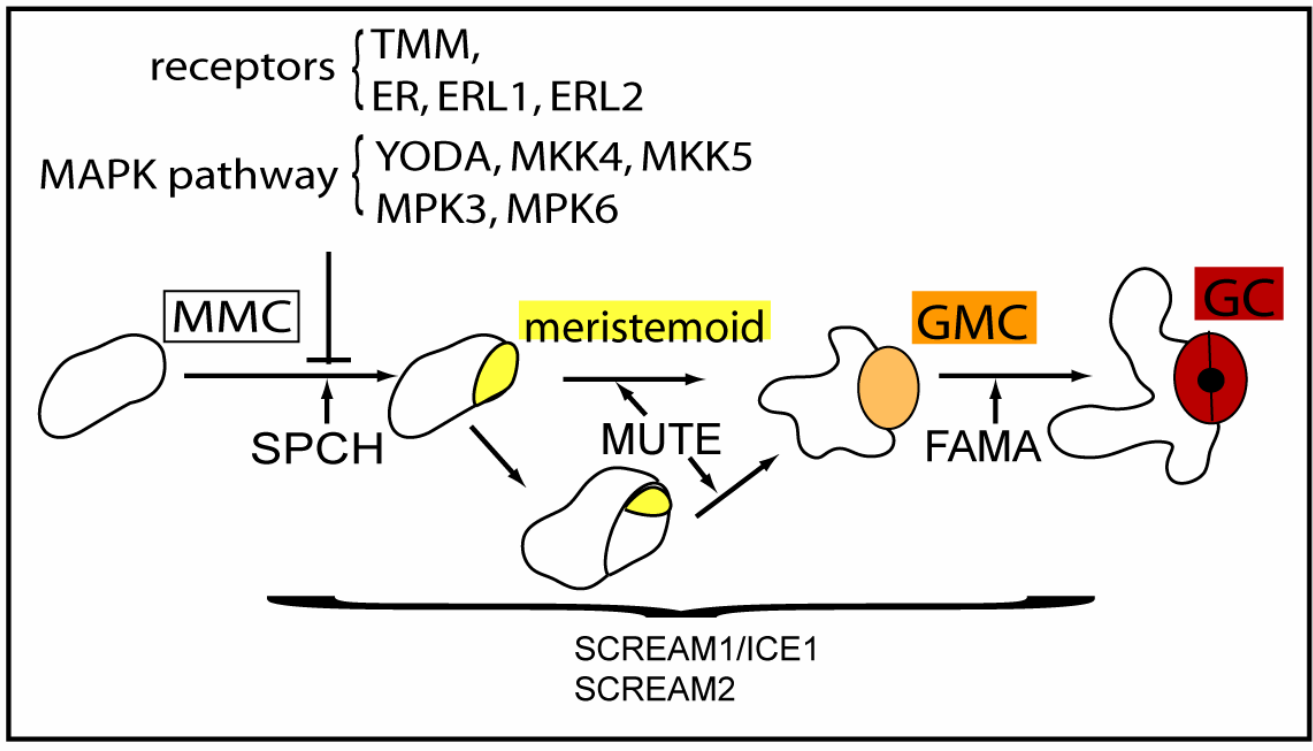


Figure S1: General pathway for Arabidopsis stomatal development. Specific cell types color-coded and names are listed to the upper right of cells: MMC (meristemoid mother cell, white), meristemoid (yellow), GMC (guard mother cell, orange) and GC (guard cell, red). Previously identified bHLH-domain containing proteins with roles in stomatal development are indicated at their points of action. SPCH regulates the MMC to meristemoid transition, MUTE the meristemoid to GMC transition, and FAMA the GMC to GC transition. Based on expression pattern and mutant phenotypes, SCREAM1/ICE1 and SCREAM 2 appear have more general roles at all stages of stomatal development. The point of opposing actions of SPCH and MAPK pathway is noted as arrow and T-bar, respectively at the MMC to meristemoid transition.

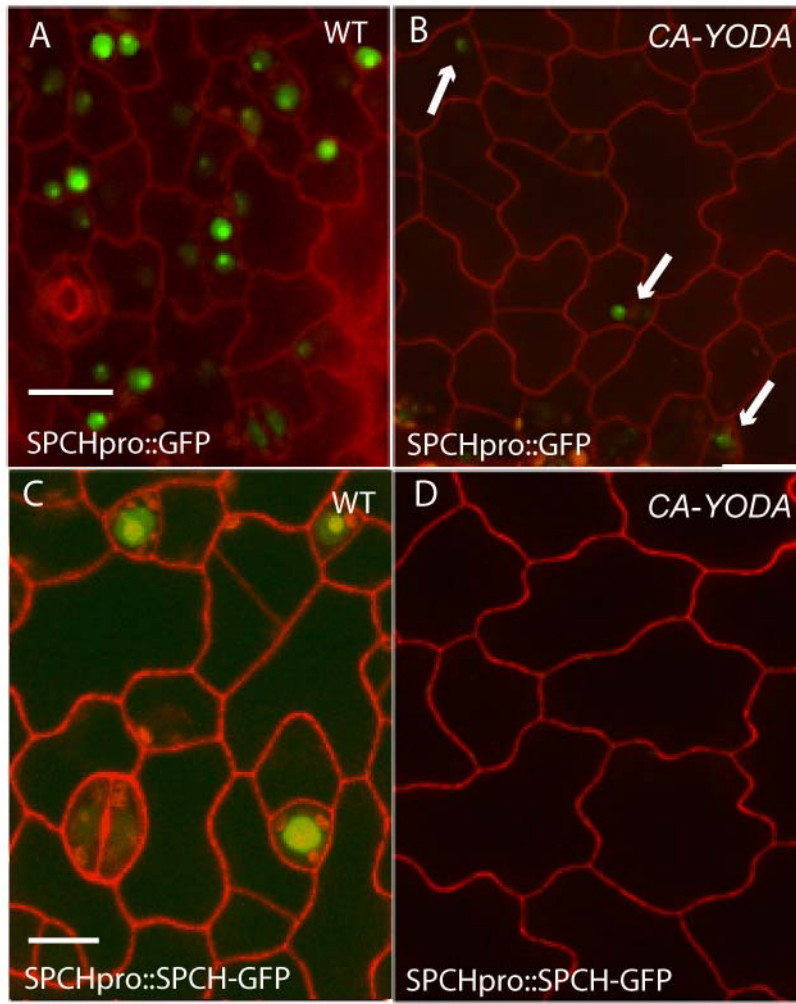


Fig. S2: Confocal images of SPCH reporters in 5-dpg cotyledons expressing constitutively active YODA (A-B) *SPCHpro::mucGFP* in (A) WT and (B) *CA-YODA* (C-D) *SPCHpro::SPCH-GFP* in WT (C) and (D) *CA-YODA*. White arrows point to GFP-positive nuclei. Chloroplasts are visible as round, brightly fluorescent red bodies in GCs and meristemoids, esp. in panel C. Images A-B and images C-D are at same magnification. Scale bar = 50 μ m

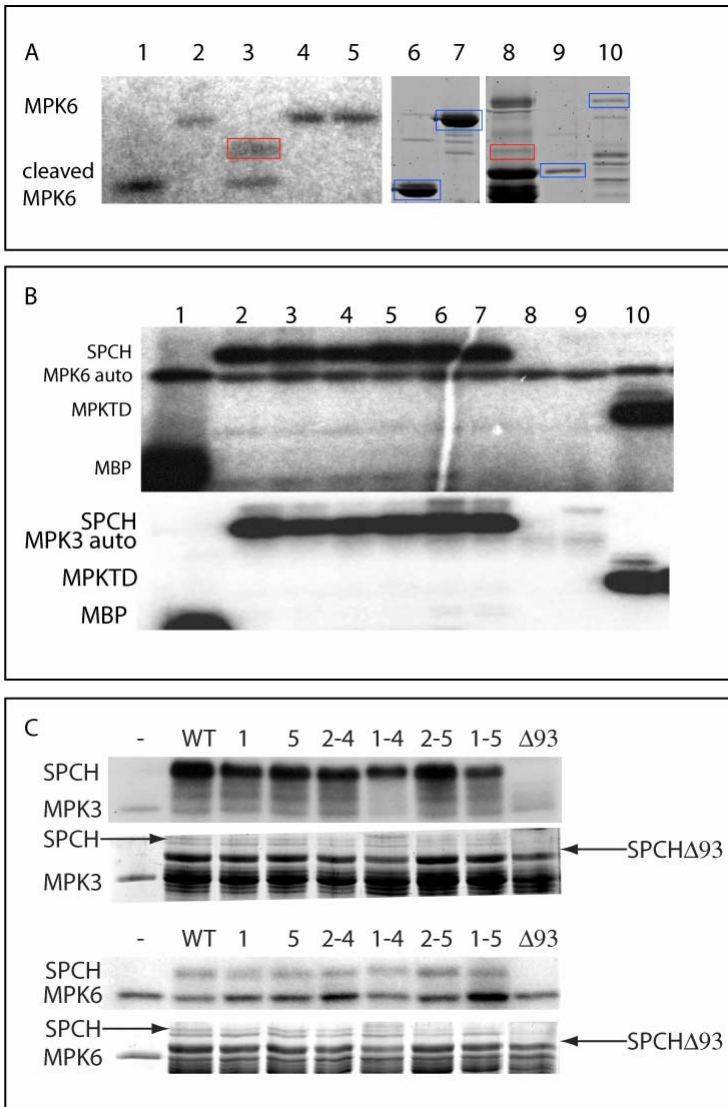


Fig S3: Additional details of in vitro kinase assays. (A) *In vitro* kinase assays illustrating that SPCH (lane 3, red box) is a substrate of MPK6 whereas MUTE (lane 4) and FAMA (lane 5) are not. GST-tagged bHLHs were subjected to *in vitro* kinase assays as described using either thrombin cleaved- or GST-tagged MPK6. Autophosphorylation of thrombin cleaved and GST-tagged MPK6 can be seen lanes 1 and 2, respectively. Panel 2 (lanes 6-10) is a SYPRO Ruby stained gel run in parallel to gel in panel 1 showing purified kinases and substrates. Bands corresponding to indicated proteins are boxed in blue (except for SPCH in red to help align with panel 1): lane 6, thrombin cleaved MPK6; lane 7, MPK6; lane 8 SPCH; lane 9, MUTE; lane 10, FAMA. Similar phosphorylation patterns are seen using MPK3 as a kinase (data not shown). (B) *In vitro* activity of MPK3 and MPK6 on SPCH variant proteins. Top panel: MPK6 activity on SPCH variants. Bottom panel: identical assay with MPK3 as kinase. Lane 1, autophosphorylation of MPK; lane 2-10 MPK incubated with SPCH variants; lane 2, SPCH; lane 3-7 SPCH with a single S/T>A change in the 1st to 5th high stringency sites, respectively; lane 8, SPCH Δ 93; lane 9, SPCH Δ 49; lane 10, MPKTD alone. (C) *In vitro* kinase assay from Fig 1 with corresponding SYPRO ruby stained gel below. Labeling as in Fig. 1.

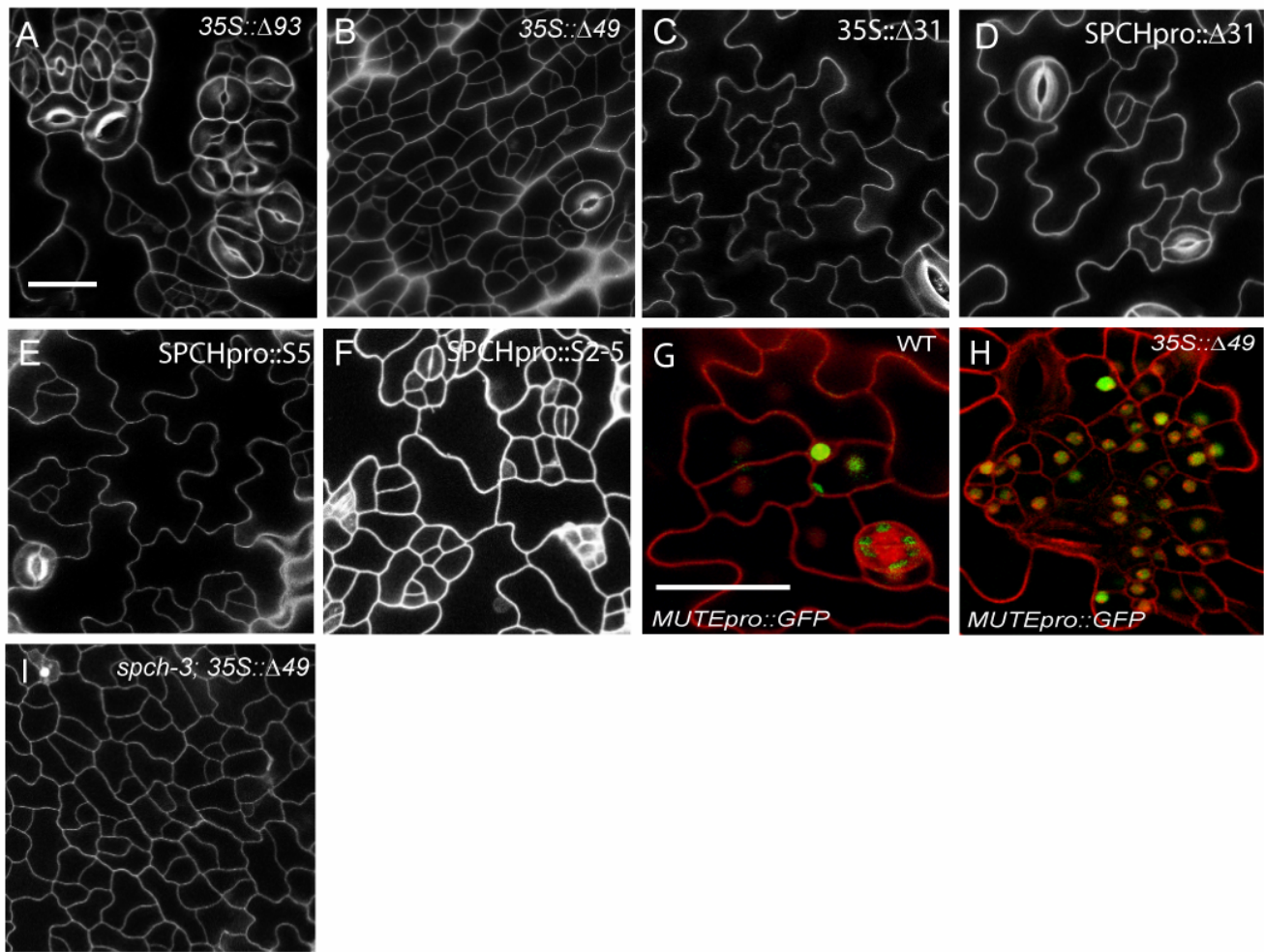


Fig. S4: Confocal images of SPCH variant phenotypes in 7-dpg adaxial cotyledons. All SPCH variants are expressed in a WT (Col) background except in panel I. (A) Stomatal clusters in *35S::SPCHΔ93* (B) Extra cell divisions in *35S::SPCHΔ49* (C) *35S::SPCHΔ31* (D) *SPCHpro::SPCHΔ31* (E) *SPCHpro::SPCHS>A5* (F) *SPCHpro::SPCHS/T>A2-5*. (G-H) *MUTEpro::nucGFP* expression in WT (G) and in *35S::SPCHΔ49* (H). I promotion of asymmetric cell division, but not stomatal formation when *35S::Δ49* is expressed in a *spch-3* (null allele) background. Cell outlines are visualized by propidium iodide staining. Images A-F (and I) and images G-H are at same scale. Scale bar = 50 μm

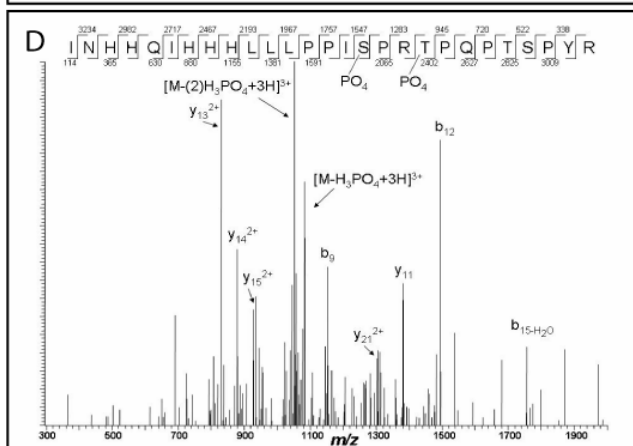
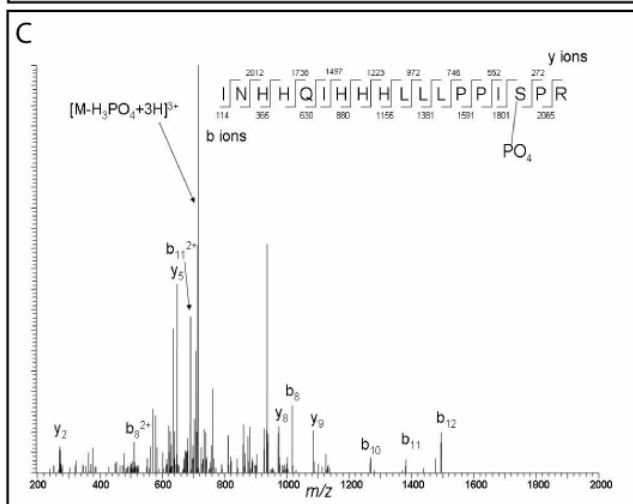
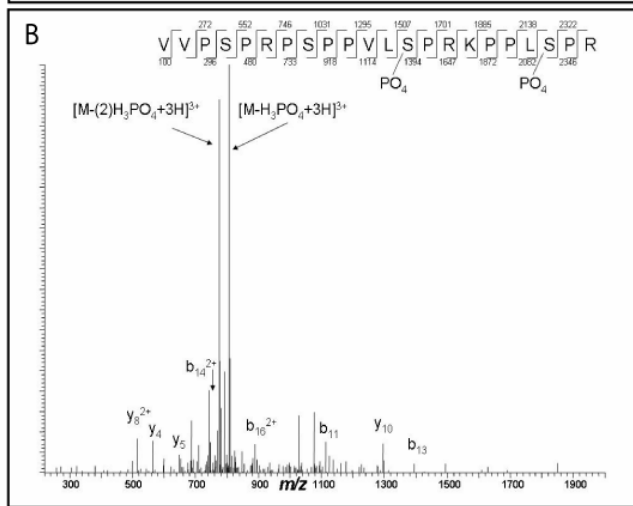
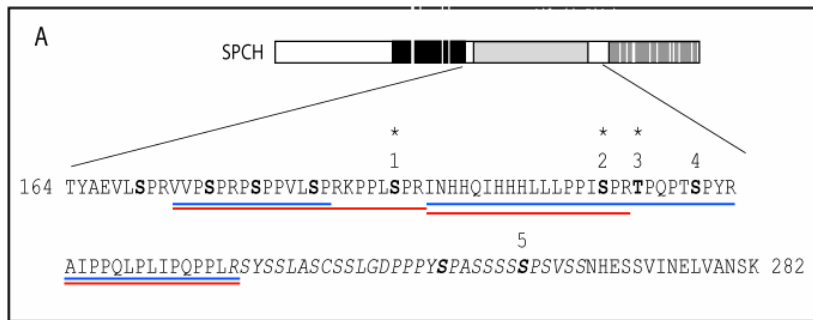


Fig. S5. Mass spectrometry identification of phosphorylated residues. A) Schematic representation of phosphorylated residues of the MPKTD. *In vitro* phosphorylated SPCH MPKTD peptide was analyzed by MS/MS analysis. Tryptic peptides identified following phosphorylation by MPK3 (blue) and MPK6 (red) were found to be phosphorylated on multiple high stringency residues (denoted by asterisks). Putative PEST domain is shown in italics. High stringency sites are: site 1 – S193, site 2 – S211, site 3 – T214, site 4 – S219 and site 5 – S255. For a complete explanation of results, see supplemental text. B) The MSMS spectra of the doubly phosphorylated triply charged SPCH peptide V174-R195. The mis-cleavage at R188 and K189 (P both N- and C-terminal to these residues) was an advantage in identifying the phosphorylation sites at both S186 and S193. The MSMS spectra clearly show prominent y mono and di-phospho losses. Additionally the y ion series, particularly y₁₀ confirms the localized serine phosphorylation sites. C) MSMS of the triply charged cation SPCH peptide I196-R213. The neutral loss is apparent, only one possible phosphorylation site is present (S211) which is confirmed by the fragment ion series. D) MSMS spectra of the mis-cleaved SPCH peptide I196-R222. The peptide was selected and fragmented as a triply charged cation. Double and single phospho losses are prominent. S211 was confirmed phosphorylated in C, it is reconfirmed here as well as the T214. Two other potential C-terminal phosphorylation sites exist (T218, S219) but the y ion series confirms the sites as S211 and T214.

<i>SPCH</i> variant	<i>Asymmetric Cell Division</i>	<i>Guard Cell Production</i>
<i>WT</i> (full length)	rescued	rescued
<i>35S::Δ93</i>	not rescued	rescued
<i>SPCHpro::Δ93</i>	not rescued	rescued
<i>SPCHpro::SPCH1-5</i>	not rescued	rescued
<i>35S::Δ49</i>	rescued	not rescued
<i>SPCHpro::Δ49</i>	rescued	not rescued
<i>SPCHpro::SPCH1-4</i>	rescued	not rescued
<i>35S::Δ31</i>	rescued	rescued
<i>SPCHpro::Δ31</i>	rescued	rescued
<i>SPCHpro::SPCH5</i>	rescued	rescued
<i>SPCHpro::SPCH2-5</i>	rescued	rescued
<i>SPCHpro::SPCH2-4</i>	rescued	rescued
<i>SPCHpro::SPCH1</i>	not rescued	not rescued

Figure S6. Rescue of two *spch* mutant phenotypes by SPCH variants

SPCH variants under control of the native promoter (and some also under the control of 35S) were tested for their ability to rescue *spch-3* null mutants. Rescue was initially assayed by following *spch-3* segregation ratios (see methods). Small pale seedlings from lines that did not produce *spch* mutants at a rate significantly different than 1:3 (not rescued) were examined microscopically for the presence of stomata or asymmetric cell divisions. Variants we previously showed mimicked *MUTE* overexpression phenotypes (Fig 2G and S4A) also appear to mimic *MUTE* in this rescue assay.

Specifically, *35S::SPCHΔ93* and *SPCHpro::SPCH1-5 S/T>A*, like *35S::MUTE*, can produce stomata in a *spch* background (14). None is capable of promoting asymmetric divisions, however, suggesting that the *35S::SPCHΔ93* and *SPCHpro::SPCH1-5 S/T>A* variants are also bypassing the step at which SPCH normally acts.

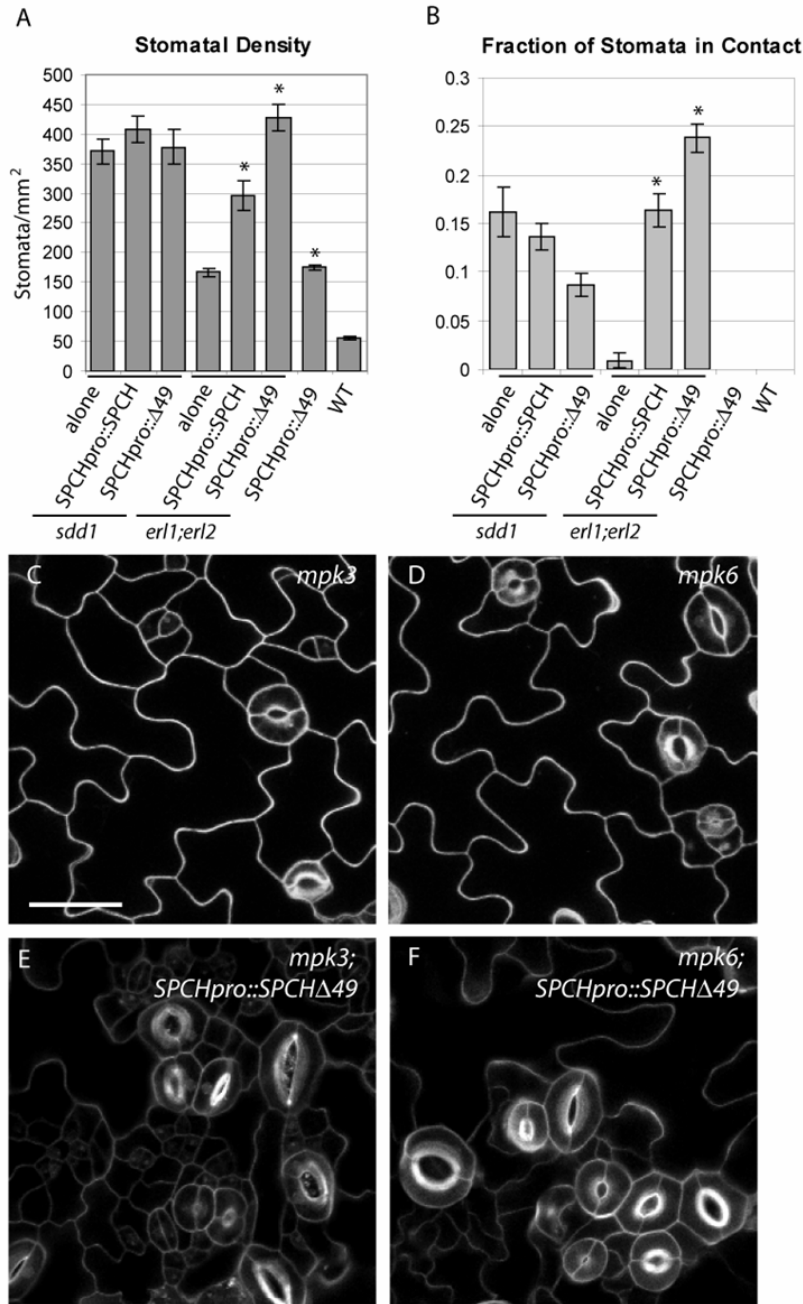


Fig. S7: Additional genetic interactions between *SPCH* and *MPK3* and *MPK6*

(A-B) Quantification of the effect of *SPCHpro::SPCH* or *SPCHpro::Δ49* on stomatal density (A) and the fraction of stomata in clusters (B) in the *sdd1* and *erl1;erl2* backgrounds. Mean \pm SE; bars marked with * are significantly different from their respective backgrounds to $P < 0.005$. (C-F) Confocal images of 7-dpg abaxial cotyledons of genotypes noted in top right corner of images. The single mutants *mpk3* (C) and *mpk6* (D) do not have a stomatal patterning phenotype. Expression of *SPCHpro::SPCHΔ49* in the *mpk3* (E) or *mpk6* (F) mutant background results in clustering of stomata. All images same scale. Scale bar = 50 μ m

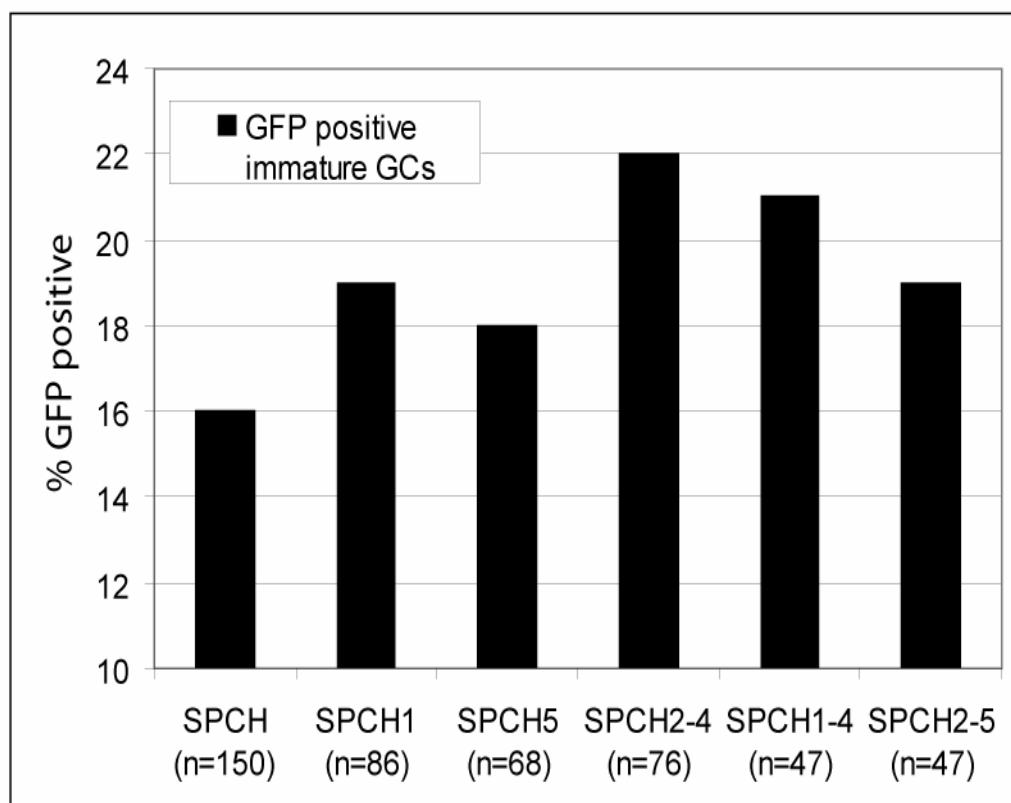


Fig. S8: Persistence of SPCH variant protein in immature GCs as a measure of endogenous protein stability. Bars represent the percentage of the total number of immature GC pairs expressing SPCHvariant-GFP/YFP. GC were considered immature if the pair had the characteristic GC shape and a pore thickening in the wall between them, but not an open stomatal pore. (n= total number of GC pairs scored)

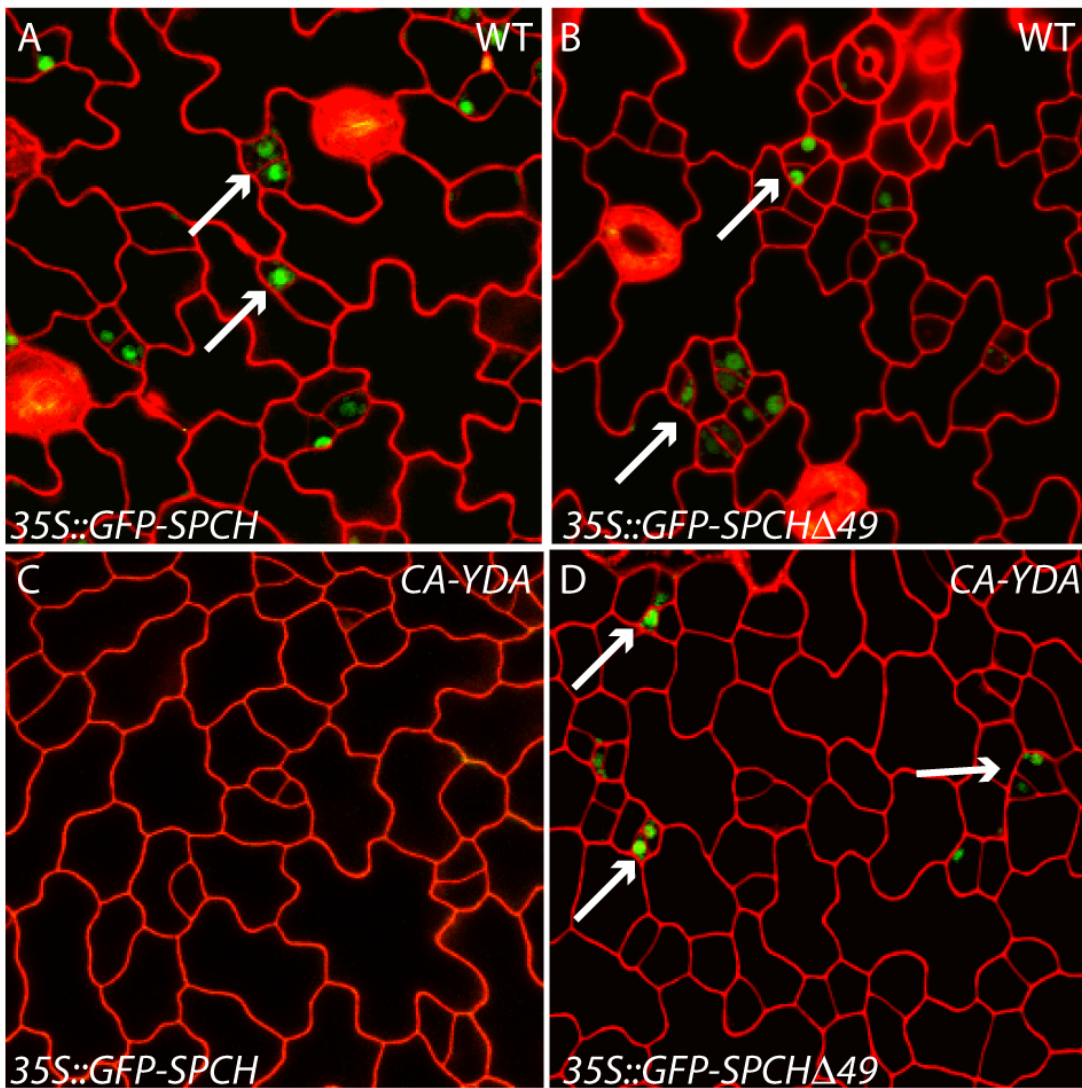


Fig. S9: Presence of SPCH and SPCH Δ 49 reporters in *CA-YDA*. (A-D) Confocal images of 3-dpg cotyledons of *CA-YDA* plants and wild type siblings. *35S::GFP-SPCH* is detectable in some cells in wild type plants (A), but, consistent with the results with the SPCH promoter (Fig. S2) it is not detectable in *CA-YDA* plants (C). SPCH Δ 49-GFP however, is detectable in both wild type (B) and *CA-YDA* (D). All images are at same magnification. Cell outlines are visualized by propidium iodide (red).

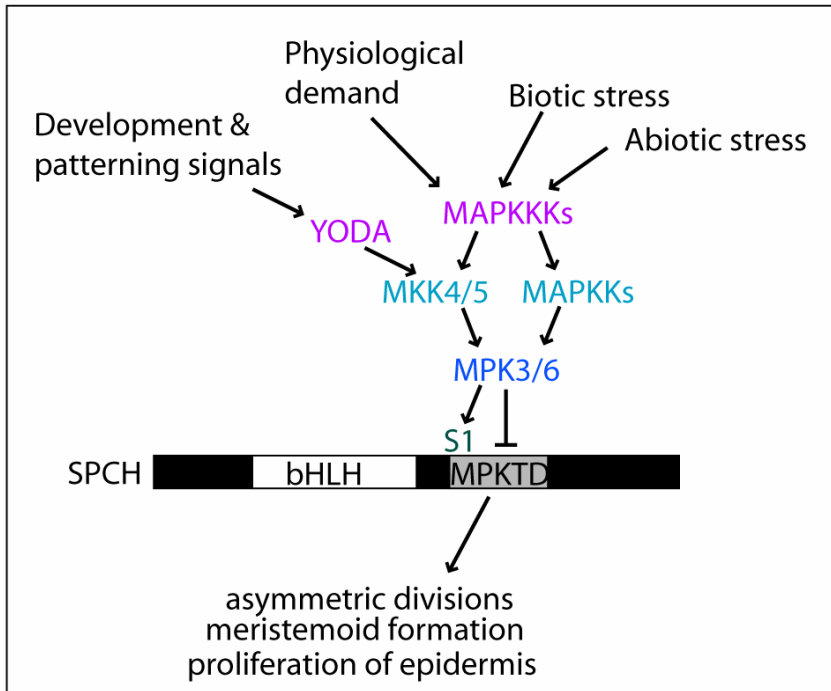


Fig. S10 Hypothetical model connecting developmental, environmental and physiological inputs to stomatal production. Under normal physiological conditions, the YODA MAPK module controls basal activity of MPK3 and MPK6. This basal activity results in SPCH being phosphorylated on site 1, which renders it active, but also on the negative regulatory sites 2-5 residues, limiting its activity to a short time period. Phosphorylation on these sites could result in inactivation of SPCH by promoting protein degradation or alternatively by altering the ability of SPCH to interact with additional stomatal regulators such as ICE1/SCREAM and/or SCREAM2. MAPK modules independent of the stomatal development module (YODA → MKK4/5 → MPK3/6) that converge on MPK3 and MPK6 can be activated by several types of upstream stimuli and this allows for fine tuning of stomatal development in response to altered biological conditions. According to this model, during acute exposure to upstream activators (e.g. pathogen attack) hyperactivation of MPK3 and MPK6 can trigger a rapid inactivation of SPCH, allowing for a reallocation of resources from developmental mechanisms to stress-tolerance, whereas in response to competing environmental demands (CO₂ levels, light, humidity) SPCH may be more or less phosphorylated allowing for alterations in SPCH activity and subtle modulation of stomatal and epidermal development programs.

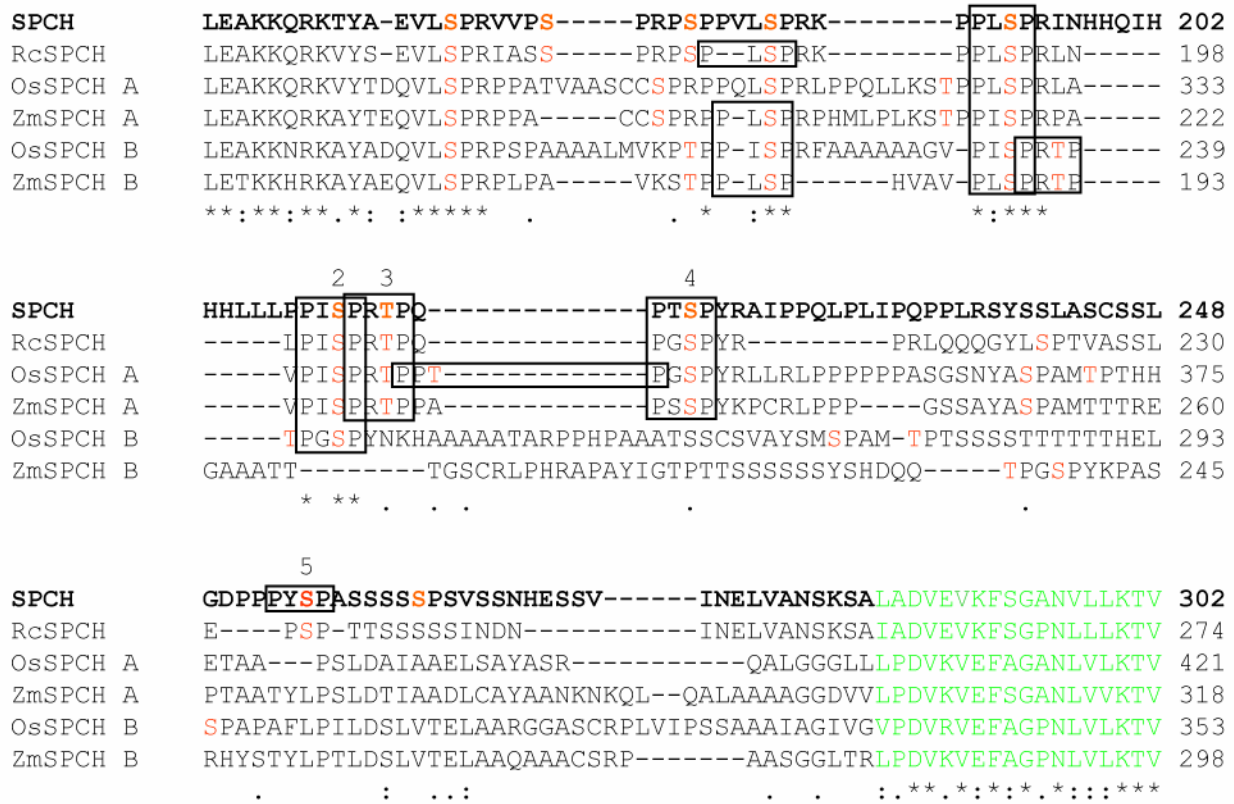


Fig. S11: Multiple sequence alignment of the MPKTD of *Arabidopsis* SPCH and its homologues from *Oryza sativa*, *Zea mays* and *Ricinus communis*.

Potential MAPK phosphorylation sites are in orange and a box surrounds high stringency sites, numbering of the high stringency sites for SPCH is as in Fig. 1A. Perfectly conserved sites are marked with ‘*’, conserved sites with ‘.’ and semi-conserved sites with ‘.’. The alignment begins after the bHLH domain. The start of the C-terminal domain is in green. TIGR database sequence identifiers are as follows: RcSPCH, 30169.m006534; ZmSPCH A, AZM5_15260; ZmSPCH B, AZM5_13800. The locus identifier for OsSPCH A is Os06g33450 and for OsSPCH B is Os02g15760. The sequence alignment was generated by ClustalW using default parameters.